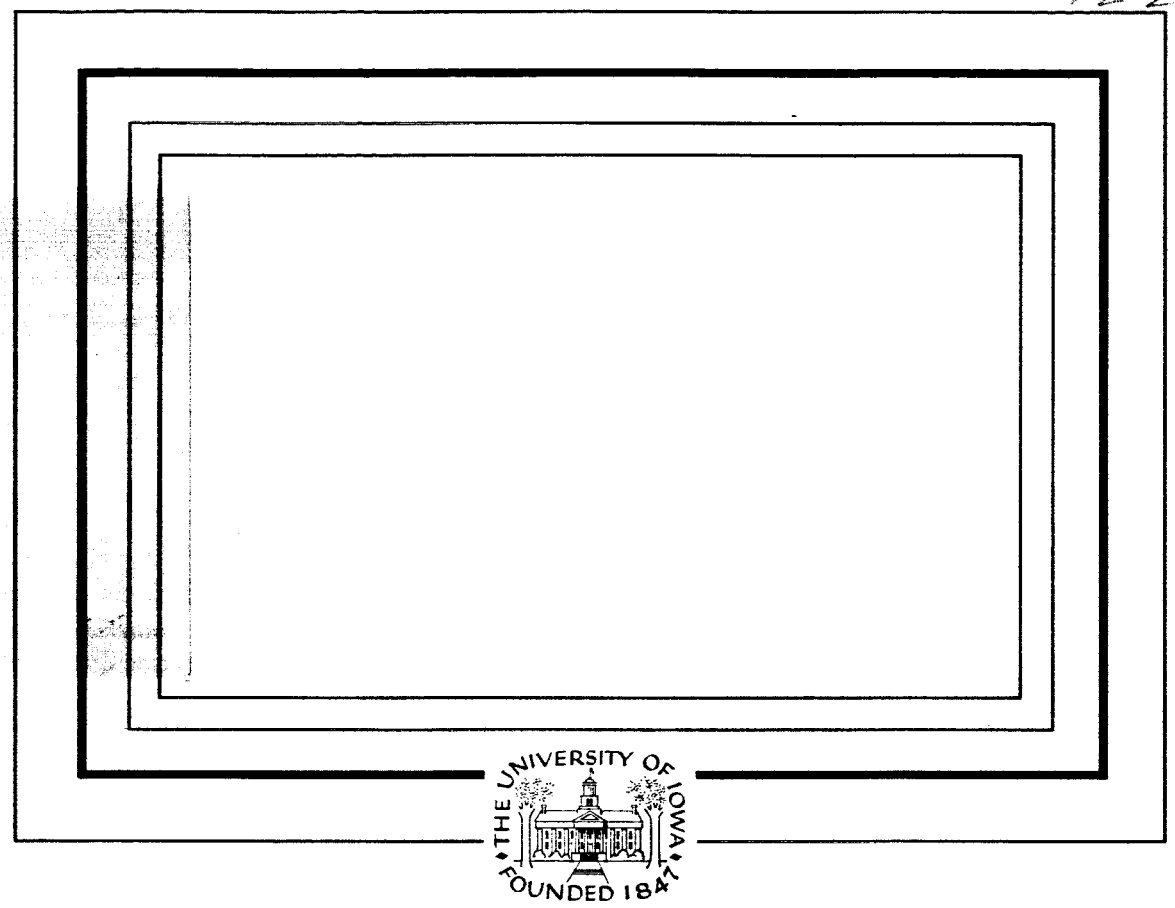

Department of Physics and Astronomy
THE UNIVERSITY OF IOWA
Iowa City, Iowa 52242

U. of Iowa 88-15

AURORAL ARCS AS MANIFESTATIONS OF MAGNETIC FRACTURES

by

Gerhard Haerendel*

Department of Physics and Astronomy
University of Iowa
Iowa City, IA 52242 USA

June 1988

* On leave from Max-Planck-Institut für Physik and Astrophysik, Institut für extraterrestrische Physik, 8046 Garching, FRG

Abstract

Properties of structured auroral arcs are derived from a model according to which magnetic energy is dominantly converted into kinetic energy of field-aligned particle beams. The free energy is stored in sheared magnetic fields inside magnetospheric-ionospheric current circuits and is taken out by spontaneous progression of the auroral acceleration region. As the process resembles the development of fractures in overstrained solid bodies, the region of energy conversion (parallel voltage) is named "fracture zone." It owes its existence to micro-instabilities excited by the associated field-aligned currents when they exceed a critical threshold. This is known to happen preferentially at altitudes of several 1000 km. The narrowness of auroral arcs is basically a consequence of the high current concentration required for instability. Their length reflects the excursions made by individual flux-tubes in the process of stress release. Parallel voltage and energy conversion rate in the fracture zone are intimately related to the thickness which also depends on the strength of the current generator or impressed magnetic shear. All basic macroscopic characteristics of the auroral acceleration region (fracture zone) are contained in and can be quantitatively derived from a simple set of equations flowing out of these global considerations. The multiplicity of auroral arcs is attributed to non-perfect matching between the nearly field-aligned current sheets and the generator. The current sheets propagating along with Alfvén speed can be described by ordinary MHD equations for most of the magnetosphere, but need kinetic corrections inside the generator and fracture zone and in an interference region between the latter and the ionosphere. The obliqueness of the current sheets is due to the transverse

progression of the fracture zone with a speed given by its thickness and the communication time with the generator. The relation of the fracture mechanism to the adiabatic "mirror resistivity" is investigated, with the conclusion that both processes tend to co-exist, but at different altitudes, the latter mainly above 2 R_E where the cold plasma contribution is negligible. The microprocesses inside the fracture zone and their macroscopic consequences are only briefly touched.

1. Introduction

Aurora borealis or the northern lights appear either as diffuse green or red glow covering parts of or the entire sky, or in a multitude of forms ranging from single diffuse or multiple thin arcs to extremely complex irregular sheets or spirals structured by rapidly moving folds and rays (or curls), by dark lanes or smoke-like clouds and subject to splitting and unfolding, brightness oscillations of various types and frequencies, and as a whole, sometimes explosively growing in intensity, expanding, and collapsing again. Some arcs are very short-lived, others appear to exist for hours. Although being continuously restructured they maintain their identity over long periods. In several decades of highly intensified auroral research by ground-based, air- and balloon-borne observations, radar probing, in situ measurements with rockets and satellites, theory and numerical simulations, enormous progress has been made in elucidating the geophysical scenery and many of the physical processes underlying the visible phenomena, in particular the global substorm events, particle beams and conical distributions, electric currents and fields, and a wide variety of wave and wave-particle phenomena. All the same it may not be unfair (in view of so much progress) to say that we are still lacking a unifying theory capable of reproducing through special solutions the morphology and dynamics of auroral displays.

The diffuse aurora, which is essentially equivalent to the losses of open plasma devices like mirror machines, is perhaps the best understood class of aurora [Ashour-Abdalla and Kennel, 1978; Ashour-Abdalla and Thorne, 1978]. Structured arcs have been theoretically approached in several ways whereby guidance by experimental exploration of the auroral source regions

played a significant role. Measurements of particle distributions, electric fields and currents [e.g., Cloutier et al., 1970; Armstrong and Zmuda, 1970; Frank and Ackerson, 1971; Gurnett, 1972; Evans, 1974; Iijima and Potemra, 1976; Shelley et al., 1976; Mozer et al., 1977, 1980; Evans et al., 1977; Croley et al., 1978; Whalen and Daly, 1979; Fennel et al., 1981; de la Beaujardière and Vondrak, 1982; Weimer et al., 1985] implied the existence of U-shaped potential structures associated with intense field-aligned currents at altitudes of several 1000 km in which the primary auroral particle beams are formed (Carlqvist and Boström, 1970; Swift, 1975, 1976]. Field-aligned potential drops distributed over thousands of kilometers seem to be often confined to narrow regions corresponding to the visible arcs. Associated with these parallel voltages are narrow (a few tens of km) structures of very strong transverse electric fields, often in pairs of opposite polarity which have been named electrostatic shocks by Mozer et al. [1977].

These observational facts and many of the associated details of particle and wave distributions impose certain constraints on a successful theoretical description, the foremost being perhaps that the acceleration regions must necessarily have narrow spatial structures capable of fast transformations. And indeed, narrow transverse scales are inherent in many of the theoretical models. Others, however, produce rather wide scales (and hence low transverse electric fields and plasma flow velocities) or are not sensitive at all to transverse structuring. A good example is the class of theories which relate the accelerating voltages in the magnetosphere to the maintenance of current continuity in converging flux-tubes when energetic electrons are the dominant current carriers. At high current densities, isotropic source

plasmas are unable to sustain the current at lower altitudes against the mirror force, and lowering of the mirror points by downward electrostatic acceleration is needed [Knight, 1973; Lemaire and Scharer, 1974; Antonova and Tverskoy, 1975; Fridman and Lemaire, 1980]. In using the current-voltage relation resulting from this effect, Lyons [1980] and Chiu and Cornwall [1980] were very successful in deriving some of the properties of auroral arcs. However, coupling this relation with an ionospheric Ohm's law in order to describe the two-dimensional potential structure, produced transverse scales of the order of 100 km. Therefore, it has often been claimed that these theories apply best to the "inverted-V" events of Frank and Ackerson [1971] and, indeed, there are striking similarities between the observed characteristics and these models. But even on much finer scales, the current-voltage relation emerging from the "mirror resistivity" is capable of reproducing observed dependencies of energy flux (and current) on the accelerating voltage [Lyons et al., 1979]. The theory obviously needs extension to smaller scales, and some attempts have been undertaken in this direction [Lyons, 1981; Lysak, 1981; Weimer et al., 1985; Chiu, 1986].

A very different class of theories considers the role of Alfvén waves as energy carriers into the acceleration region [Mallinckrodt and Carlson, 1978; Goertz and Boswell, 1979; Haerendel, 1980, 1983; Lysak, 1981; Lysak and Dum, 1983; Goertz, 1984]. Narrow transverse scales involve kinetic effects and are associated with parallel electric fields. These kinetic Alfvén waves [Hasegawa, 1976; Goertz, 1984] are, therefore, capable of transforming electromagnetic energy into parallel particle beams and do so on transverse scales on the low side of the observed spectrum of arc widths.

Besides the kinetic effects of propagating waves, current instability has been regarded as one of the prime causes of parallel electric fields at high altitudes [Block and Fälthammar, 1968; Carlqvist and Boström, 1970; Kindel and Kennel, 1971; Mozer, 1976; Papadopoulos, 1977; Hudson et al., 1978; Fälthammar, 1978; Haerendel, 1980, 1983; Lysak and Dum, 1983] and many attempts have been made to relate the parallel fields and voltages to the excited turbulence and associated anomalous resistivity. Narrow transverse scales emerge mostly from the need of current concentration and range between multiples of the electron and ion inertial lengths.

Other approaches are only mentioned briefly, because they are farther away from the subsequently developed concept. Swift [1976, 1979] investigated two-dimensional double layers in a kinetic approach and suggested that the gyro-radius of ions accelerated by the full voltage across the double layer be the fundamental transverse scale. In Sato's [1978] feedback instability model involving the oscillation of energy (derived from convection motions) between conjugate ionospheres, the width of and/or spacing between auroral arcs is a product of Pedersen drift and bounce-time of the Alfvén waves.

The approach taken in this paper starts from an earlier developed concept [Haerendel, 1980; 1981] that the region of current instability is not only the site of conversion of electromagnetic into kinetic energy of field-parallel beams, but also plays an active role in extracting magnetic energy stored in a magnetospheric-ionospheric current circuit. Its function is compared with that of a *fracture* developing in a solid body under shear stresses. The fracture zone ($\hat{=}$ acceleration region) releases magnetic tensions as it progresses transverse to $\underline{B}$ and with respect to the rest frame of the

plasma. Alfvén waves communicate the event all along the field-lines and transport the magnetic energy from high altitudes into the fracture zone. Therefore, these waves are not impressed from the ultimate energy source (current generator), but emitted from and attached to the fracture zones. Some details of this model have changed since 1980. Most importantly however, energy conservation on the macro-scale has been added, which proved to be most useful in deriving simple relations for transverse fields, parallel voltages and energy deposition rates [Haerendel, 1988]. All these quantities depend strongly on the thickness of the region of instantaneous energy deposition, the fracture zone. This thickness is the focus of the present paper. After a summary of the main features of the fracture model [Haerendel, 1988] in Section 2, we will address the relative (Section 3) and absolute (Section 4) transverse scale lengths implied by this model. In Section 5 we will look into the impact of the interaction between emitted Alfvén waves and current generator on the structure (mainly the multiplicity) of auroral arcs. In Section 6 we will check the appropriateness of the used macroscopic description vis-à-vis kinetic effects. Section 7 presents an attempt to reconcile the current instability/Alfvén wave picture with the mirror resistivity concept. It is concluded that they are likely to coexist, the latter one being confined to higher altitudes, i.e., the transmission medium between generator and fracture zone. Finally, only brief comments on the physics of the fracture zone are added in Section 8. Most of the preceding conclusions are derived by considering this region essentially as a "black box." It is obvious that this creates severe shortcomings, whose removal requires much further work on the basic microscopic processes and their macroscopic consequences.

2. The Fracture Model

The field-parallel voltages developing at several 1000 km altitude above auroral arcs and the energy dissipated there, mostly by electron and ion beam production, are considered in the context of the overall current circuit. Per unit cross-section of a flux-tube, typically one order of magnitude more energy is dissipated above an auroral arc than elsewhere inside the current loop. This fast drain of energy from the circuit has to be balanced somehow. The fracture model is based on the assumption that this occurs by propagation of the acceleration region ($E_{\parallel} \neq 0$) into the interior of the current circuit thereby tapping the reservoir of free magnetic energy which exists in form of stressed magnetic field.

The magnetospheric-ionospheric current circuit depicted in Figure 1 is driven by forces, $\underline{F}_G$, (out of the plane) which cannot be balanced locally by magnetic normal stresses, but rather by shear stresses which are transmitted along the magnetic field via field-aligned currents and taken up by ion-neutral friction in the upper atmosphere. This final transfer to the neutral gas is effected by the Pedersen current which closes the circuit in the ionosphere. Hence, there is a continuous flux of shear momentum from the upper magnetosphere into the ionosphere as a result of which the plasma is convecting at relatively low speed in the direction dictated by the generator forces, $\underline{F}_G$. This situation may exist for some time without any accompanying generation of auroral arcs (there may be some diffuse aurora, just due to participation of hot magnetospheric electrons). By processes not specified here, however, the field-aligned current, in particular its upward directed component, may become concentrated to the extent that some part of it

becomes unstable at greater heights above the ionosphere [Kindel and Kennel, 1971], develops anomalous resistivity of some kind and then sustains a field-parallel potential drop. The thus created zone of $E_{\parallel} \neq 0$ with its drastically enhanced dissipation is normally very narrow in comparison with the width of the overall current circuit. The field-parallel voltage, $V_{\parallel}$, decouples the stressed field above it from the ionosphere and allows fast transverse motions which, after a few transit times of an Alfvén wave, τ_A, between the height of $E_{\parallel} \neq 0$ and the generator, lead to a reduction, if not complete removal of the shear stresses [Haerendel, 1988]. This is connected with a release of energy. The energy stored in a particular flux-tube flows out within a few transit times, τ_A. If the process has not died out after that, it can only continue to exist, because the zone of $E_{\parallel} \neq 0$ is propagating into the stressed field region, i.e., into the interior of the circuit which still contains free magnetic energy. This concept can explain how auroral arcs maintain their identity for times much longer than τ_A ($\cong$ 100 s). Motions of the arc with respect to the plasma would be witnesses of such a process (observational evidence will be covered in a subsequent paper). However, it may happen as well that current concentration and field-aligned voltage generation occur because of enhanced action of the generator. In this case, the propagation of the acceleration region would be directed so as to widen the circuit and thus accommodate the enhanced influx of energy (minus the dissipated part) [Haerendel, 1987].

Altogether the analogy of the process with a fracture developing in a stressed solid body is obvious. A most important consequence is that the

propagation into (or out of) the current circuit is led by the $E_{\parallel} \neq 0$ region, the "fracture zone." If d is the width, its normal propagation speed, v_n, is given by:

$$v_n = \frac{d}{2\tau_A} \quad , \tag{1}$$

where

$$\tau_A = 2 \int_F^G \frac{d\ell_{\parallel}}{c_A} \quad . \tag{2}$$

c_A is the parallel group velocity of an Alfvén-wave, and the integral in Equation 2 is performed between fracture zone (F) and generator (G). (The factor 2 is chosen because at least two periods τ_A are needed for the interaction with the generator (compare Figure 2).) v_n/c_A is a very small number. As the fracture zone propagates, it causes a lateral displacement of the (unstable) field-aligned current sheet. This displacement is communicated along the magnetic field with the elastic speed of the medium, the Alfvén velocity c_A. This is why τ_A is the fundamental time-constant of the process. Owing to the lateral displacement the formerly purely field-aligned (force-free) current acquires a transverse component caused by the inertia of the ions which become exposed to the induced electric field. In brief, the fracture zone creates slightly oblique current sheets and thus sets the plasma into motion as a current sheet is passing by. The transverse electric field corresponding to this motion, $\underline{E}_{\perp} = - \underline{v}_{\perp} \times \underline{B}/c$, switched on by passage of a sheet current, J_F, is:

$$E_{\perp,m} = R_w \cdot J_F \quad , \tag{3}$$

where

$$R_w = \frac{4\pi c_A}{c^2} \tag{4}$$

is the wave impedance.

After the current perturbation has reached the generator and interacted with it (see Section 5), a second current sheet of opposite inclination with respect to $\underline{B}$ (reflected wave) will switch off the electric field, $\underline{E}_\perp$. This is, however, not the end of the process; the plasma must not only be displaced in one direction. In the low altitude magnetosphere, the magnetic field is very strong,

$$\beta = \frac{8\pi p}{B^2} << 1 \quad . \tag{5}$$

No magnetic flux can pile up anywhere. Therefore, all motions must be of the interchange type. This means there must be an opposite, nearly equal displacement of the plasma. This is achieved by a third wave exchanged between generator and fracture zone which applies an oppositely directed field, $\underline{E}_\perp$. This field is finally switched off by a fourth current sheet. The basic structure of these oblique current sheets attached to the fracture zone and interacting with the generator is sketched in a greatly simplified fashion for the case of a homogeneous zero order field in Figure 2. There are a number of

details that will become clearer in later sections. The equipotential lines are not continued towards higher altitudes, because the field is not electrostatic (switched on and off by induction) and can only be approximated by a potential field over a limited height range.

The details of emission and reflection of the current sheets from the fracture zone go beyond the scope of this paper (see Section 8). What is essential in the present context is to realize that the parallel voltage is necessarily flanked by regions of high $\underline{E}_\perp$ of opposite sign. The integrals

$$V_\perp = \int E_x \cdot dx \simeq E_{\perp,m} \cdot \frac{d}{2} \tag{6}$$

on either side are of almost equal magnitude (except for the small ionospheric voltage across an arc), but of opposite sign and equal to the maximum voltage along $\underline{B}$:

$$V_{\parallel,max} \simeq V_\perp = |E_{\perp,m}| \cdot \frac{d}{2} \quad . \tag{7}$$

The bell-shape of the fracture zone ($E_\parallel \neq 0$) in Figures 1 and 2 is a consequence of the matching of $E_\parallel$ in its interior to $\underline{E}_\perp$ in the attached oblique current fronts in combination with the dependence of $E_\perp$ on the integrated current (Equation 3) and the assumption of constant current density, $j_\parallel$.

As we relate the appearance of $V_\parallel$ to a current driven anomalous resistance, we have to specify the threshold for instability, j_{crit}. The microphysics of such current driven turbulence is extremely complex [Sagdeev and Saleev, 1969; Kindel and Kennel, 1971; Mozer, 1976;

Papadopoulos, 1977; Hudson et al., 1978; Rowland et al., 1981; Lotko, 1986]. We will not deal with it except by postulating that the critical threshold of the relative velocity between electrons and ions, c_{crit}, lies somewhere above the ion acoustic speed, c_s:

$$j_{crit} = en\,c_{crit} = f \cdot en\,c_s \quad . \tag{8}$$

f depends on the ratio of ion and electron temperatures and on the type of waves which are most instrumental in exchanging momentum between ions and electrons. Very good candidates are the ion-acoustic solitons found by Temerin et al. [1982] with the S3-3 satellite and confirmed by the Viking-data of Boström et al. [1987] (see also Hudson et al. [1983] and Lotko [1986]).

f may be of the order of 10 (up to $\sqrt{m_i/m_e}$), but need not be constant throughout the fracture zone, since in the course of its development, temperature and density change considerably (see Section 8). If we treat f as a constant, we do so for the sake of simplicity. By detailed comparisons of the quantitative predictions of the fracture model with observations, one can develop a tool for assessing effective values of f.

Finally, we can close the set of relations by assuming that the unstable current settles somewhere close to j_{crit}. Hence, the sheet current density, J_F, of Equation 5 can be estimated to be:

$$J_F \simeq j_{crit} \cdot \frac{d}{2} \quad . \tag{9}$$

With this expression we can rewrite the parallel voltage

$$V_{\parallel,max} \simeq R_w j_{crit} \frac{d^2}{4} \tag{10}$$

and express the dissipation rate per unit cross-section of a flux-tube, $\dot{\varepsilon}_l$, by:

$$\varepsilon_{\parallel,max} \simeq j_{crit} \cdot V_{\parallel,max} = R_w j_{crit}^2 \frac{d^2}{4} \quad . \tag{11}$$

Much of $\dot{\varepsilon}_l$ consists in production of field-aligned electron and ion beams (run-away particles). But some fraction is converted into heat of the background plasma whose main role is to maintain charge neutrality and participate in the overall momentum balance (see Section 8).

The foregoing relations demonstrate clearly the great dynamical importance of the thickness, d. It controls the transverse motion, $c\,E_\perp/B_0$, above the fracture zone, which leads to stress release. It further controls the propagation speed of this zone and thereby the energy conversion rate, $\dot{\varepsilon}_l$, and transverse and parallel voltages. For the remainder of this paper we will focus on this quantity.

3. Relative Thickness

The fracture model of auroral acceleration links the transverse electric fields (named "electrostatic shocks" by Mozer et al. [1977]) intimately to the field-parallel accelerating voltages. It is the near-equality of the magnitudes of transverse and parallel voltages (Equation 7) that provides an easy means of determining the latter. A determination of $V_{\parallel}$ on the basis of current density and effective resistivity would be a very difficult task. In this respect (and not only in this) the "fracture process" in low beta plasmas is analogous to reconnection in high beta plasmas. Also there, the processes around the neutral (x-) line or "diffusion region" in collisionfree plasmas have remained fairly obscure until today, whereas the role of the attached intermediate waves and slow shocks has been much better explored and has led to quantitative conclusions. The oblique current fronts emitted by the progressing fracture zone (or reflected from it after interaction with the generator plasma) transfer transverse or tangential momentum to the plasma. The magnitude of that momentum or tangential velocity, $\underline{v}_{\perp}$, solely depends on the integrated sheet current traversing a plasma element and the wave impedance, R_w, but not on the obliqueness, i.e., the angle between the current front and the magnetic field, which is arc tan (v_n/c_A) and as such extremely small. The motion with $\underline{v}_{\perp}$ has the meaning of implementing the stress relief. So, it is fundamental to the overall energy conversion. However, the kinetic energy contained in this motion serves only as an *intermediate energy storage*. When the whole (multiple) current front has passed and the plasma has essentially come to rest again, much of this energy has flown as Poynting flux into the acceleration region (fracture zone) which made the

stress relief possible (through decoupling from the ionosphere). Most of the energy is being dumped into particle beams, which carry it out of this region.

Auroral arcs exhibit the spatial extent of the acceleration region. This region is at least as long as required for completing the stress relief motion. The speed of stress relief is:

$$\underline{v}_\perp = c \frac{\underline{E}_\perp \times \underline{B}}{B_0^2} \quad . \tag{12}$$

As a current sheet with integrated current density, J_F, passes by, $E_\perp$ builds up and decays subsequently through the following sheet. A reasonable estimate for the average stress relief motion is therefore:

$$\overline{v}_\perp = \frac{1}{2} c \frac{E_{\perp,m}}{B_0} \quad . \tag{13}$$

The total excursion of a plasma element (along the direction of the arc) is experienced during the time interval, $2\tau_A$, because it needs two complete wave transits to the generator and back for switching $E_\perp$ on and off. Hence, this excursion (mostly in longitude) is given by:

$$s = \overline{v}_\perp 2\tau_A = c_A \tau_A \cdot \frac{2\pi j_{crit} d}{c B_0} \tag{14}$$

(this follows immediately from Equations 3, 4, 9, and 13). If we, furthermore, make use of Equation 8 and introduce the ion plasma frequency, ω_{pi}, at the level of the fracture zone, we can convert this expression into:

$$\frac{d}{s} = \frac{2\,\frac{c}{\omega_{pi}}}{c_{crit} \cdot \tau_A} \quad . \tag{15}$$

If we assume a stationary situation, this relation provides us with a lower limit for the ratio of thickness to length of an auroral arc. Of course, this implies proper projection from the level of the fracture zone ($\sim 1\ R_E$) to the ionosphere, whereby it should be remembered that distances in latitude and longitude project slightly differently, but essentially $\propto (B_F/B)^{1/2}$. An arc could be longer, i.e., d/s smaller than implied by Equation 15. If the fracture zone is characterized by a temperature of a few eV and f in Equation 8 is of order 10, c_{crit} is of the order of 100 km/s. $\tau_A \approx 100$s and $c/\omega_{pi} \approx$ 20-70 km ($\hat{=}\ n_F = 100\text{-}10\ cm^{-3}$ of H^+). So, $d/s < 10^{-2}$. A stationary arc of, say, 5 km visual width should extend for at least 500 km. This is quite consistent with reality.

In general, the ratio d/s decreases with increasing temperature and density, mostly because higher current concentration is needed in order to pass the threshold for instability, j_{crit}. In stellar magnetic fields with much higher plasma density, we expect therefore much more extreme values of d/s. When we now ask ourselves why auroral arcs are so thin, we would answer on the basis of the fracture model: "because they represent the displacement of field-lines in the process of stress relief through electrostatic decoupling from the ionosphere and because this decoupling is possible only in sheets of highly concentrated field-aligned current."

4. Absolute Thickness

The thickness of the fracture zone ($E_\parallel \neq 0$) is at least 2d, since four current sheets, each of width d/2 (Equation 9) and Figure 2, are the minimum number required to switch on and off the attached, oppositely directed transverse electric fields. The incompressibility of $\underline{B}$ or near-electrostatic nature of $\underline{E}$ imply continuity of the electrostatic potential lines from fracture zone into the adjacent portions of the wave field.. More complex structures of the fracture zone are thinkable. Since the potential drop parallel $\underline{B}$ varies strongly across the region and since the visible light emission sensitively depends on the energy of the primary electrons, the visible arc would appear thinner than the projected thickness of the fracture zone ($E_\parallel \neq 0$) in the ionosphere. Probably a factor of 0.5 is not a bad estimate. Hence, one scale-length, d_F, projected into the ionosphere would be a close measure of the thickness of the visible phenomenon.

$$d_{Arc} \simeq \sqrt{\frac{B_F}{B_{ion}}}\, d_F \tag{16}$$

The total unstable current is $2d_F j_{\perp F} \approx 2d\, j_{crit} = 4\, J_F$. It connects to the generator current, $j_{\perp G}$, whose integrated density (in a symmetric magnetosphere only one half is counted)

$$J_G = \frac{1}{2} \int j_{\perp G}\, d\ell_\parallel \tag{17}$$

may exceed that supplied by the unstable current sheet in question. Assuming *steady state* and projecting J_F to the level of the generator:

$$4 J_F \sqrt{\frac{B_G}{B_F}} = q_c J_G \quad . \tag{18}$$

$q_c \leq 1$ is a measure of the completeness of current closure between the nearly field-aligned auroral current and the transverse generator current. Using Equation 9 and the total transverse field component $B_{\perp G}$, inside the current circuit but near the generator:

$$B_{\perp G} = \frac{4\pi J_G}{c} \quad , \tag{19}$$

we can express d_F as:

$$d_F = \frac{q_c}{2} \cdot \frac{c\sqrt{B_F B_G}}{4\pi j_{crit}} \cdot \frac{B_{\perp G}}{B_G} \quad . \tag{20}$$

This way of writing relates the thickness, d_F, clearly to the properties of the generator plasma. The relative strength of the magnetic tensions balancing the generator forces, $\underline{F}_G$, is contained in $B_{\perp G}/B_G$. How much of the total field-aligned current communicating these stresses to the upper atmosphere is actually involved in the particular unstable auroral current sheet (fraction q_c), is a question of the history of stress build-up and current

concentration and falls outside the scope of this paper. However, there are two upper limits:

$$q_c \leq 1 \quad , \quad \frac{B_{\perp G}}{B_G} \lesssim 1 \quad . \tag{21}$$

Whereas the first one is obvious, the second one has to do with the postulate that the stressed field should at least constitute of stable magnetic configuration. If the pressure due to the transverse component exceeds that of the unperturbed field in which the current loop is imbedded, stability is hard to imagine [Parker, 1974] (unless there is direct interaction with a super-Alfvénic flow). Probably the sheared field would break out of its configuration and assume a state of lower energy. $B_{\perp G}/B_G$ is also related to the plasma beta (Section 5). The inequalities in Equation 21 then constitute an upper limit for d_F:

$$d_F = \frac{c\sqrt{B_F B_G}}{4\pi j_{crit}} \cdot r \tag{22}$$

with

$$r = \frac{q_c}{2} \frac{B_{\perp G}}{B_G} \lesssim 0.5 \quad . \tag{23}$$

Let us assume that the current instability (fracture) occurs in a field, B_F, of 0.06 G, a density of 100 cm^{-3} (H^+) and a temperature of 1 eV. For the field

inside the generator, B_G, we adopt 30 nT. With f = 10, $j_{crit} \cong 2.2\ \mu A/m^2$ and $d_F \lesssim 76$ km. This upper limit projected to the level of auroral displays (100 km altitude) becomes about 25 km, i.e., substantially greater than typically observed arc widths. This indicates that either the primary field tensions are well below their conceivable upper limit ($B_{\perp G} \ll B_G$) or the total field-aligned current belonging to one particular circuit is more widely distributed ($q_c \ll 1$), or both. We will discuss this point further in the following section.

The expression of Equation 22 for d_F leads to a particularly transparent expression for field-aligned voltage, $V_\parallel$, and dissipation rate, $\dot{\varepsilon}_\parallel$ (Equations 10 and 11):

$$eV_{\parallel,max} = \frac{c_A}{c_{crit}} \cdot \frac{B_F B_G}{4\pi n_F} \cdot \left(\frac{r}{2}\right)^2 \tag{24}$$

$$\dot{\varepsilon}_\parallel = j_\parallel V_\parallel = \frac{B_F}{B_G} \cdot c_A \frac{B_G^2}{4\pi} \cdot \left(\frac{r}{2}\right)^2 . \tag{25}$$

Free magnetic energy $B_G^2/4\pi\cdot(r/2)^2$ flows in the form of Poynting flux along the magnetic field into the fracture zone and becomes focussed by the convergence of the field (B_F/B_G). It balances the dissipated energy, $\dot{\varepsilon}_\parallel$. Dividing $\dot{\varepsilon}_\parallel$ by the critical current, $en_F c_{crit}$, gives the parallel voltage. This is the way $\dot{\varepsilon}_\parallel$ and $V_\parallel$ were derived in [Haerendel, 1988]. It should also be pointed out that $E_\perp$ and the mean stress relief velocity, $v_\perp$, assume a very sipmle form when expressed by Equation 7, 13, 22, and 24:

$$E_{\perp,m} = \frac{c_A}{c}\sqrt{B_F B_G} \cdot \frac{r}{2} \tag{26}$$

$$v_\perp = \sqrt{\frac{B_F}{B_G}} \cdot c_A \cdot \frac{r}{4} \ . \tag{27}$$

We proceed to illustrate the quantitative implications of the preceding relations by looking at the numerical values of $eV_\parallel$ and $\dot{\varepsilon}_\parallel$ for the choice of parameters given above. We obtain:

$$eV_\parallel = 825\,\text{keV} \cdot \left(\frac{r}{2}\right)^2$$

and

$$\dot{\varepsilon}_\parallel = 1.9 \cdot 10^3\,\text{erg/cm}^2\text{s} \cdot \left(\frac{r}{2}\right)^2 \ .$$

So, if we want to explain the existence of a parallel voltage of 5 kV, we would have to choose $r = 0.16$. This yields $\dot{\varepsilon}_{\parallel,F} \cong 12$ erg/cm^{2}s, $d_F \cong 20$ km, and $v_n = 10^2$ m/s ($\tau_A = 10^2$ s). Projected to the 100 km level, $\dot{\varepsilon}_\parallel \cong 100$ erg/cm^{2}s, $d_{Arc} \simeq 7$ km and $v_n = 35$ m/s. The very low magnitude of v_n should be noticed. It would appear as relative velocity of an arc with respect to the ionospheric plasma above the E region (measurable, for instance, with Thomson scatter radar and, in fact, observed [to be published]). The typical amplitude of the transverse electric field of the so-called "electrostatic shocks" [Mozer et al., 1977] would be ≈ 0.4 V/m and $v_\perp \approx 70$ km/s. Measurements of $E_\perp$ are thus particularly suited to evaluate the least accessible quantity, r. All above

values appear to be entirely consistent with reality, but we must remember that most of the underlying equations are simple estimates. The results should therefore be taken with some caution; a factor of two is probably a good estimate for the inherent uncertainty of quantitative deductions.

5. Multiplicity of Arcs

So far we regarded stationary situations in which the fracture zone propagates steadily into the current circuit extracting free magnetic energy. It is, however, likely that in most cases the Alfvén waves carrying the nearly field-aligned current and the dynamics of the generator plasma driving the unperturbed current do not match. There will be partial reflection creating oscillations of the current sheets between generator and fracture zone with fundamental period, τ_A, (Equation 2), and consequently, also an oscillatory progression of the fracture zone. In this section, we will examine the interaction of current sheet and generator in a simplified and incomplete fashion. The lack of completeness is a consequence of our neglect of the complex physics of the fracture zone at this stage of investigation.

Figure 3 shows a detail of Figure 2, the interface between a current sheet emerging from the auroral acceleration region with the generator plasma. In reality, there is no clear separation between generator and passive propagation medium. The hot plasma of the tail plasma sheet or dayside boundary layers reaches towards medium and lower altitudes because of pitch-angle diffusion. However, the convergence of the flux-tubes has the effect that most of the power fed into a current loop closing through the ionosphere originates between about $\pm 30°$ from the equator. The magnetic field in this region may increase by a factor of 3 to 6 from its minimum value, but it is distinctly different from the field near the fracture zone which is by about two orders of magnitude larger. Hence, we feel justified to regard the generator as being concentrated in a finite region near the equator with average field-strength, B_G. This region is shown in the top section of Figure 3.

The propagation medium is shown only close to the generator. The variation of B and c_A along the field-lines will be worked in later.

The current, j_l, flowing behind the front attached to the "nose" of the fracture zone (see Figure 2) connects to the generator current, $j_{\perp G}$. We consider an equilibrium situation that existed before set-up of the fracture process and still prevails inside the current circuit (to the right of the current front in Figure 2), in which pressure gradient forces are balanced by magnetic tensions:

$$-\frac{\partial p_o}{\partial y} + \frac{j_{G0} B_G}{c} = 0 \qquad (28)$$

(y-coordinate out of plane). The plasma is in a state of steady convection. The corresponding electric field is determined by closure of the current $\int j_{G0}\, d\ell_l$ through the ionosphere with its intrinsic resistance (inverse Pedersen-conductance). Since we are only interested in simple estimates, we assume that $\partial p_0/\partial y$ does not vary much in y-direction (out of plane) and can be characterized by p_0 and a gradient length, L_p:

$$j_{G0} = \frac{c p_0}{B_G L_p} \qquad (29)$$

As the current front propagates with respect to the plasma's rest frame in v_n - (x -) direction following the fracture zone, the transverse current is being reduced:

$$j_G(t) = j_{G0} - \frac{j_\parallel v_\parallel t}{\ell_G} \quad , \tag{30}$$

where ℓ_G is the effective extent of the generator from the plane of symmetry (only one hemisphere considered). For simplicity, we regard $j_\parallel$ as constant and redistribute the current instantaneously and uniformly over the width, ℓ_G, of the generator. Introducing the characteristic time-scale, τ_c, for current closure:

$$\tau_c = \frac{j_{G0}\ell_G}{j_\parallel v_n} = \frac{j_{G0}}{j_\parallel v_n} \tag{31}$$

and the perturbed pressure of the generator plasma:

$$p_1(t) = p_0 - p_G(t) \quad , \tag{32}$$

we obtain a simple (linearized) equation of motion for the generator (at a fixed position in the undisturbed plasma frame or normal coordinate, x):

$$\dot{v}_G = \frac{p_0}{L_p \rho_G} \cdot \frac{t}{\tau_c} - \frac{p_1}{L_p \rho_G} \quad . \tag{33}$$

Here we made use of Equations 29 and 30 and assume that the gradient scale of p_1 equals that of p_0. ρ_G is the mass density inside the generator.

The plasma is set into motion because of the gradual reduction of the balancing magnetic shear stresses, as the current front passes by. The kinetic energy of this motion is derived from a decrease of the plasma's interval

energy (pressure decrease, $p_1 > 0$). Furthermore, a Poynting flux carries energy away from the generator. If we neglect the change of magnetic energy inside the generator, most of it being stored in the propagation medium between generator and fracture zone, and assume homogeneity in flow direction (i.e., neglect any divergences in y-direction), we obtain a simple expression for energy conservation:

$$\frac{\partial}{\partial t}\left(\frac{1}{2}\rho_G v_G^2 + \frac{p}{\gamma - 1}\right) = E_{\perp G} \cdot j_G \tag{34}$$

γ is the ratio of specific heats. In a generator necessarily $E_{\perp G} \cdot j_G < 0$. This is equivalent to an energy loss by Poynting flux along $\underline{B}$ ($\underline{S} \sim \underline{E}_\perp \times \underline{B}_\perp$). Setting:

$$E_{\perp G} = -\frac{1}{c} v_G B_G \tag{35}$$

we obtain with Equations 28-32:

$$\frac{\partial p_1}{\partial t} = (\gamma - 1)\left[\frac{\partial}{\partial t}\left(\frac{\rho_G}{2} v_G^2\right) + \frac{p_0}{L_p}\left(1 - \frac{t}{\tau_c}\right) v_G\right] .$$

Assuming incompressibility ($\dot{\rho}_n = 0$) and introducing $\dot{v}_G$ from Equation 33, we get a very simple relation for the build-up of the pressure perturbation, p_1:

$$\dot{p}_1 = (\gamma - 1)\frac{p_0 - p_1}{L_p} v_G . \tag{36}$$

Equations 33 and 36 describe the dynamics and energetics of the generator plasma in response to progressive current closure. Figure 4 is a sketch of the fate of an individual flux-tube in this process. Note that our model assumes homogeneity in flow direction, i.e., a whole current sheet acts in unison. As the magnetic tensions are reduced, the plasma moves in the direction of the unperturbed force thereby reducing the plasma pressure. Eventually, the pressure force falls below the remaining tensions, the motion slows down, and is even reversed. Formally, this is seen from the second order differential equation following from Equation 33 and 36:

$$\ddot{v}_G + (\gamma - 1)\omega_G^2\left(1 - \frac{p_1}{p_0}\right)v_G = \omega_G^2 \frac{L_p}{\tau_c} \quad . \tag{37}$$

ω_G is the fundamental acoustic frequency of the generator plasma:

$$\omega_G = \sqrt{\frac{p_0}{\rho_G}} \cdot \frac{1}{L_p} = \frac{c_{SG}}{\sqrt{\gamma} L_p} \quad . \tag{38}$$

Without the nonlinear term, p_1/p_0, which introduces damping, Equation 37 yields oscillatory solutions for v_G with frequency ω_G and amplitude:

$$v_{G,max} = \frac{2}{\gamma - 1} \frac{L_p}{\tau_c} \quad . \tag{39}$$

It is not necessary to obtain numerical solutions of the nonlinear equation (37), in order to discuss the dynamical properties of the system and derive some general conclusions. The generator is characterized by two time-scales, τ_c and ω_G^{-1}. In addition, we must regard the communication time, τ_A, of generator and fracture zone. As argued in Section 4, it takes four Alfvén travel times, τ_A, for full interaction of an unstable current sheet with the generator. Dividing the r.h.s. of Equation 31 by $4\,\tau_A$, introducing the projection factor $\sqrt{B_G/B_F}$ for a current sheet between fracture zone and generator and using Equation 18, one finds:

$$\tau_c = \frac{4}{q_c}\,\tau_A \quad . \tag{40}$$

Incomplete current closure, $q_c < 1$, prolongs τ_c and reduces the maximum velocity attained by the generator. $q_c = 1$, on the other hand, may allow a displacement of the generator plasma by a distance comparable to L_p (multiply Equation 39 by $4\,\tau_A$), which means full extraction of the internal energy in one interaction. The generator plasma comes to rest, a single auroral arc has been formed.

Whether this actually happens or not is a question of *dynamical matching*. This matching is perfect, if $\omega_G\tau_A \approx 2/\pi(\approx 1)$. In one oscillation period of the generator, the internal energy is reduced to a degree corresponding to the jump of $B_{\perp G}$ from one to the other side of the interacting current sheet. It is not necessary that this current sheet closes the generator current completely, i.e., $q_c < 1$ is possible. Thus, for $\omega_G\tau_A \approx 1$ energy would not slosh several times between generator and fracture zone.

This is not so for $\omega_G \tau_A$ much different from unity. In the case of $\omega_G \tau_A \gg 1$, not all of the free energy available is extracted in one oscillation period of the generator. Several periods pass during the transit of the current sheet. This means that the current will split into several parallel sheets of the same sense, and the fracture zone accordingly. Hence, we are led to presume that multiple auroral arcs are set up, closely spaced, i.e., by distances of order of their width. Such multiple band structure of auroral arcs is indeed frequently observed.

In the opposite case of $\omega_G \tau_A \ll 1$, the current sheet passes in much less than one oscillation period. Again, not all available energy has been released. But now this energy will be used to build up another current circuit, by stressing again (although to a lesser extent) the magnetic field. Whether this newly built-up circuit develops current instability and arc formation or not depends on the current concentration process and is outside our considerations. It can be seen, however, that the mean energy flux out of the generator in this case is less than the Poynting flux drawn from release of the magnetic tensions between fracture zone and generator. Temporal modulations of the deposited energy (auroral brightness) would be the result.

By far the simplest situation exists for complete current closure and perfect dynamical matching (this case is depicted in Figure 2). Only one arc would exist and d would be given by Equation 22 with $r = 0.5\ (B_{\perp G}/B_G)$. But more often the generator current, J_G, seems to connect to the ionosphere in a widely distributed current, $j_\parallel$, arising from the history of energy build-up at the generator and its interaction with the ionosphere. Current concentration may lead to instability in some part of the circuit. Once such instability has

been set up, the propagation of the fracture zones ensures its maintenance and may even sweep up some hitherto subcritical part of $j_{\parallel}$. But mostly $q_c < 1$. Often, the enhanced energy release by arc formation may be more than balanced by new energy supply to the generator. Then the current circuits can expand (not shrink) while accommodating the additional energy influx. Multiple arc systems (not to be confused with the small-scale splitting of one arc into several parallel bands) may thus be part of one larger current system. The smallness of parameter r in Equations 22-27 would be mainly attributed to $q_c \ll 1$, the maximum possible number of parallel arcs being q_c^{-1}. Five to ten parallel arcs, each of them only several km wide (visual width) and spaced irregularly over the region of field-aligned current, are consistent with this view, and for $B_{\perp G} \lesssim B_G$ exhibit voltages and energy fluxes as observed. In checking this statement with the help of Equations 22-27, the reader should keep in mind that the choice of parameters in Section 4 is not unique. For instance, n_F may be well below 100 cm^{-3}, which would lower j_{crit} and enhance d and $V_{\parallel}$ for equal value of r.

A numerical evaluation of $\omega_G \tau_A$ will help us to judge what properties of the generator would make perfect dynamical matching possible. If the generator plasma consists dominantly of ionized hydrogen,

$$\omega_G = 0.05\ s^{-1} \cdot \left(\frac{kT_G}{1\ kev}\right)^{1/2} \cdot \left(\frac{1\ R_E}{L_p}\right) \quad . \tag{41}$$

In the plasma sheet, $kT_G \approx$ 5-10 keV. Since τ_A is typically longer than 100 s, it needs pressure scales, L_p, of the order of 10 R_E or more to yield $\omega_G \cdot \tau_A \approx 1$.

Such scales appear to be entirely possible, but often they may be smaller. This means that $\omega_G \cdot \tau_A$ is well above unity, and multiply banded arcs should occur frequently.

One can relate the matching condition to the relative magnetic shear stresses by:

$$\frac{1}{c} J_G B_G = \frac{B_{\perp G}}{B_G} \cdot \frac{B_G^2}{4\pi} = \frac{p_0 \ell_G}{L_p}$$

which leads to:

$$\frac{B_{\perp G}}{B_G} = \frac{\beta_G}{2} \frac{\ell_G}{L_p} \tag{42}$$

with $\beta_G = 8\pi p_o/B_G{}^2$. With c_{AG} being the Alfvén velocity inside the generator, ω_G can be written as:

$$\omega_G = \sqrt{\beta_G} \frac{c_{AG}}{L_p} \cdot \tag{43}$$

These two relations can then be combined to yield:

$$\frac{B_{\perp G}}{B_G} = \frac{\sqrt{\beta_G}}{4} \cdot \omega_G \tau_{AG} \cdot \tag{44}$$

Here τ_{AG}, the travel time of an Alfvén wave through the generator ($2\ell_G/c_{AG}$), replaces τ_A, the travel time between fracture zone and generator. Naturally,

$\tau_{AG} < \tau_A$, but not much smaller, since c_A increases rapidly outside the generator. Large values of $\omega_G \tau_A$ can thus be quite consistent with strong field distortions ($B_{\perp G} \approx B_G$), if $\beta_G \ll 1$. On the other hand, since β_G is typically of order 0.3 - 0.5 in the plasma sheet, perfect matching would imply $B_{\perp G}/B_G$ to lie well below unity.

None of these considerations imply a structure of auroral arcs that would be inconsistent with observations. On the contrary, the existence of multiple structured arcs, often several inside one large-scale current system, is a natural outcome of these considerations. $q_c \ll 1$ may also be the condition for the existence of "inverted V" events of typically 100 km width [Frank and Ackerson, 1971].

6. Thickness and Kinetic Scales

Alfvén waves carry the message about "fracture" along the field-lines to the generator, Alfvén waves transport the magnetic energy into the fracture zone where it is dissipated (mostly by generation of parallel beams). It is, therefore, interesting to see what kind of Alfvén waves are suggested by the fracture model which is of macroscopic nature and derives the transverse scales from current threshold, closure at the generator and its dynamics. Small transverse scales affect the dispersion relation of Alfvén waves [Hasegawa, 1976; Goertz and Boswell, 1979]:

(a)
$$\frac{\omega}{k_\parallel} = c_A \sqrt{1 + k_\perp^2 \rho^2} \quad \text{for } \beta > \frac{m_e}{m_i} \tag{45}$$

and

(b)
$$\frac{\omega}{k_\parallel} = \frac{c_A}{\sqrt{1 + k_\perp^2 \frac{c^2}{\omega_{pe}^2}}} \quad \text{for } \beta < \frac{m_e}{m_i} \tag{46}$$

where $\rho = \rho_i \sqrt{T_e/T_i + 3/4}$ and ρ_i = ion gyroradius. Such *kinetic Alfvén waves* are dissipative by virtue of their parallel electric field component. Hence, some of the energy extracted from the current circuit may already be dissipated before it has reached the fracture zone. Therefore, we must check what Equation 22 implies on the nature of these waves.

The expression for $d_{\parallel}$ can be rewritten as:

(a) $$d_F = \rho_i \cdot \frac{1}{\beta_F} \cdot \frac{r}{f}\sqrt{\frac{B_G}{B_F}} \qquad (47)$$

or:

(b) $$d_F = \frac{c}{\omega_{pe}} \cdot \sqrt{\frac{m_i}{m_e \beta_F}} \cdot \frac{r}{f}\sqrt{\frac{B_G}{B_F}} \qquad (48)$$

The Alfvén waves are kinetic if

$$\beta_F \gtrsim \frac{r}{f}\sqrt{\frac{B_G}{B_F}} \qquad \text{case (a)}$$

or

$$\beta_F \gtrsim \frac{m_i}{m_e} \cdot \frac{r^2 B_G}{f^2 B_F} \qquad \text{case (b)}$$

The foregoing considerations imply $r \approx 10^{-1}$, $f \approx 10$, $\sqrt{B_G/B_F} \approx 10^{-1}$. Hence $\beta_F \gtrsim 10^{-3}$ is required. With the parameter set used in Sections 3 and 4, $\beta_F \approx 10^{-6}$. This says that the oblique Alfvén waves which carry the current between fracture zone and generator are of sufficiently large width in order to neglect kinetic effects, at least at lower levels of the magnetosphere. Inside the generator, however, where β approaches unity, the projected value of d can

come close to the ion gyroradius and the propagation speed of the waves may be better described by Equation 45.

The short travel time of Alfvén waves between fracture zone and the ionosphere, $\tau_{A\ell}$, in conjunction with the high reflectivity of the latter [Scholer, 1970], leads to many reflections and an interference pattern of very narrow transverse scale (see Figure 2). With $d_F \approx 10$ km, $\tau_A \approx 100$ s and $\tau_{A\ell} \approx 2$ s, the transverse scale turns out to be of the order of 100 m, well below c/ω_{pe} for $n_F = 100\ cm^{-3}$. For the description of these waves, a kinetic approach appears necessary and damping by electron acceleration parallel $\underline{B}$ may be important. Although only small potential differences of order $(\tau_{A\ell}/\tau_A)\cdot V_i \approx 100$ V, exist across these scales, parallel heating of the electrons may have rather interesting consequences (e.g., excitation of ion cyclotron waves and production of ion conical distributions at low altitudes).

7. Relation to Mirror Resistivity

At first sight, the fracture model of parallel acceleration and the concept of "mirror resistivity," i.e., the maintenance of current continuity against the mirror force acting on hot, current carrying electrons, seem to be mutually exclusive. The first involves current instability in the presence of a dominant population of cold plasma and turbulent scattering of at least a large fraction of the particles (except a run-away component), whereas the second is based on adiabatic motion of the energetic current carriers with no cold plasma background. If there were such a background, the current-voltage relation of Knight [1973], Antonova and Tverskoy [1975], and Fridman and Lemaire [1980] would be drastically changed. Indeed, it is hard to imagine how this second effect can operate below about 2 R_E altitude, in densities above 10 cm^{-3}, since even the highest observed current densities, if entirely maintained by energetic electrons, correspond to less than 1 cm^{-3} at heights above 1 R_E. Either beam or current driven instabilities will lead to some momentum exchange between the energetic electrons and the background plasma. If an electric field parallel to $\underline{B}$ exists, it does so for reasons other than lowering the mirror points of the energetic particles. On the other hand, at greater heights, i.e., above about 2 R_E, the mirror effect may well operate and maintain a noticeable voltage along the lines of force.

We proceed to estimate possible voltages at greater height by coupling the current-voltage relation of Knight [1973], Antonova and Tverskoy [1975] and Fridman and Lemaire [1980] in the approximation

$$j_\parallel = K V_\parallel \tag{49}$$

with our expression for energy conservation (Equation 25). Equation 49 is valid for $1 \ll eV_l/W_e \ll B/B_G$, where W_e is the energy of the hot source electrons (from the generator (G)). We anticipate that only part of the Poynting flux (fraction a_E) is consumed in maintaining the voltage $V_{l,m}$ above, say, geocentric distances of 3 R_E. So, we insert Equation 49 on the l.h.s. of Equation 25, while multiplying its r.h.s. by a_E (< 1). The result is:

$$V_{l,m} = \sqrt{a_E} \cdot \frac{c_{A3}}{c} \sqrt{B_3 B_G} \cdot d_m \cdot \frac{r}{2} \quad . \tag{50}$$

Index "3" refers to the lower height limit of effective mirror resistivity ($r \gtrsim 3\ R_E$), and d_m is a characteristic length used already by Lysak [1981]. Since

$$K = \frac{e^2 n_{eH}}{\sqrt{2\pi m_e W_e}} \tag{51}$$

has the dimension of a conductance per unit area, the product of K with the local wave impedance, $R_{w,3} = 4\pi\, c_{A3}/c^2$, has the dimension of an $(\text{area})^{-1}$, and:

$$d_m = \left(R_{w,3} K \right)^{-1/2} \quad . \tag{52}$$

n_{eH} and W_e are density and mean energy of the hot electrons at the level of the generator plasma.

If we generalize Equation 22 for the width of a current sheet by replacing j_{crit} by j_l from Equation 49 and refer to 3 R_E, we find:

$$d_3 = \frac{2}{\sqrt{a_E}} d_m \quad . \tag{53}$$

The remarkable feature of this relation is that d_3 does not depend on the parameter r (Equation 23) which contains properties of the generator; only the fractional energy deposition rate, a_E, enters.

We evaluate d_3 and $V_{\parallel,m}$ by choosing popular values for the involved parameters: $W_e = 0.5$ keV, $n_{eH} = (0.3 - 1.0)$ cm^{-3} [Fridman and Lemaire, 1980; Lyons, 1980], and $n_3 = 1$ cm^{-3} ($\hat{=} c_{A3} = 4 \cdot 10^9$ cm/s). This leads to values of K and d_m ranging from 0.033 to 0.11 esu and 7.3 to 4.0 km, respectively, and potential drops $V_{\parallel,m} = (35\text{-}19)\ \text{kV} \cdot \sqrt{a_E} \cdot r$. Lysak [1981] proposed that d_m constitutes a critical damping width for Alfvén waves impinging from high altitudes. Longer wavelengths are essentially transmitted, shorter ones are strongly damped and do not reach lower altitudes. This is quite consistent with the view adopted here, with the refinement that the actual width, d_3, depends on the fractional energy deposition above 3 R_E, a_E, (Equation 53). Knowledge of the relative strength, r, of the generator provides an estimate of the potential drop above 3 R_E (Equation 50).

Interesting conclusions can be drawn if we postulate that indeed both processes operate simultaneously, the mirror resistivity effect above about 3 R_E and the fracture process below. An auroral arc would be a joint product of both acceleration processes. Hence, its width must be consistent with both, d_F (Equation 22) and d_3 (Equation 53):

$$d_{Arc} = \sqrt{\frac{B_F}{B_{ion}}}\, d_F = \sqrt{\frac{B_3}{B_{ion}}}\, d_3 \quad . \tag{54}$$

Since $d_F \propto r$ and $d_3 \propto (a_E)^{-1/2}$, Equation 54 yields an expression for $\sqrt{a_E}\cdot r$, the combination that appears in the relation for $V_{\parallel,m}$. This is no surprise because it reflects the current-voltage relation (Equation 49) worked into the expression for d_3. Equation 54 only specifies the value of $j_\parallel$ to be used in this relation, and yields:

$$V_{\parallel,m} = \frac{B_3}{B_F} \cdot \frac{j_{crit}}{K} \quad . \tag{55}$$

Inserting the values used in Section 4 for j_{crit} (0.67 esu) and in this section for K (0.033 - 0.11 esu), and with $B_3/B_F = 0.31$, we obtain $V_{\parallel,m} = 1.9$ kV for the low density case ($n_{eH} = 0.3$ cm^{-3}) and $V_{\parallel,m} = 0.6$ kV for $n_{eH} = 1.0$ cm^{-3} (in the expression for K). If we want to explain a standard auroral arc with 5 keV primary electrons, we have to evaluate the relation for $V_{\parallel,F}$ (Equation 24) by subtracting $V_{\parallel,m}$ and relating it to an energy influx (r.h.s.) reduced by $(1 - a_E)$. Hence, we have two relations for combinations of a_E and r which can be easily solved. With the above values we obtain the numbers listed in Table 1.

Table 1: Potential drops in fracture zone ($V_{\parallel,F}$) and above 3 R_E ($V_{\parallel,m}$) with corresponding values for relative energy deposition above 3 R_E (a_E), relative strength of generator (r) and width of auroral arcs (d_{Arc}) for a total voltage of 5 kV.

$n_{e,H}$	K	$V_{\parallel,m}$	a_E	r	d_{Arc}
0.3 cm^{-3}	0.033 esu	1.9 kV	0.16	0.14	7.4 km
1.0 cm^{-3}	0.11 esu	0.6 kV	0.04	0.15	8.4 km

Although many different choices of parameters could be made, these numbers are quite illustrative. The width of the auroral arcs and the relative strength of the generator, r, follow mainly from our choice of 5 kV for the total potential drop and j_{crit}. It is satisfying that standard values for $V_\parallel$ and j_{crit} are capable of producing reasonable thicknesses as well as values of r consistent with Equation 23. The distribution of energy consumption and voltage over the two regimes varies significantly, with the tendency that the by far greatest portion of the inflowing energy is dissipated in the fracture zone, which also contains the major potential drop.

The outcome of this comparison of both acceleration mechanisms is that they are likely to coexist with varying relative importance. Narrow scales, as reflected by auroral arcs, are genuine to both mechanisms, if one adopts the view of nearly complete decoupling from the ionosphere. The new element of the present treatment of mirror resistivity is that we combined the current-voltage relation with an energy conservation equation rather than with Ohm's law of the ionosphere [Lyons, 1980; Chiu and Cornwall, 1980], to obtain

a new expression for the transverse scale (Equation 53). The main remaining questions pertain to the ratio of beam particles emerging from the fracture zone to background plasma (or trapped particles) and to the reasons underlying the observed quadratic relation between energy flux and voltage which is so easily derived from a purely adiabatic theory, i.e., from the current-voltage relation of Equation 49 [Lyons et al., 1979; Lyons, 1980]. This cannot be attacked in this paper. It involves the micro- and macrophysics of the fracture zone.

8. Remarks on the Fracture Zone

Although the existence of a region of anomalous current dissipation at several 1000 km altitude is the key element of the here considered concept of linear acceleration in a collisionless, low beta plasma, we were able to draw many conclusions without specifying the dissipation process, nor its immediate local consequences. Likewise, we could derive a propagation speed (v_n) of this region without knowing its transport properties (e.g., diffusivity). All this flows mainly from energy conservation and the properties of the attached Alfvén waves. What we cannot specify, however, is the height extent of the fracture zone. It is determined by the effective resistivity, η^*, through:

$$\Delta h_F = \frac{V_\parallel}{\eta^* j_{crit}} \quad . \tag{56}$$

With our standard numbers, $V_\parallel = 5$ kV and $j_{crit} = 2.2\ \mu A/m^2$, we find: $\eta^* = 360\ \Omega m \cdot (1\ R_E/\Delta h_F)$. This may be interpreted in terms of an effective collision frequency, ν^*, through:

$$\eta^* = \frac{4\pi\nu^*}{\omega_{pe}^2} \quad . \tag{57}$$

Setting $\Delta h_F = 1\ R_E$, in accordance with observations of ion and electron beams above auroral arcs, we find $\nu^* \cong 10^3\ s^{-1} \hat{=} 0.08\ \omega_{pi}$. Such a value of ν^* is entirely reasonable, but does not say what kind of waves are instrumental in providing resistivity [Sagdeev and Galeev, 1969; Papadopoulos, 1977; Hudson et al., 1978; Rowland et al., 1981; Lotko, 1986]. One of the most promising

candidates for these waves are the small confined double layers or ion-acoustic solitons measured by Temerin et al. [1982] and Boström et al. [1987]. Although these findings suggest a stepwise potential drop, these steps are so small ($\sim kT_e/e$) and so large in number that from the macroscopic point of view η^* is smoothly distributed. However, η^* is not an intrinsic property, but intimately related to $j_\parallel - j_{crit}$ [Lysak and Dum, 1983]. As the dissipation process affects the value of j_{crit}, this quantity is subject to evolution during passage of the fracture zone.

The reason for referring to these very simple assessments of an effective resistivity or collision frequency is that we want to compare local transport and heating rates with the macroscopically determined parameters of the fracture zone.

$$D_m = \frac{c^2 \eta^*}{4\pi} \tag{58}$$

is the magnetic diffusivity connected with η^* and

$$\tau_F = \frac{d_F^2}{D_m} \tag{59}$$

the characteristic time-scale for transverse current redistribution or diffusion of $B_\perp$ inside the fracture zone. Of course, on its outside where the current is stable, η^* and D_m are practically equal to zero. Taking η^* from above and $d_F \cong 20$ km we obtain $\tau_F \approx 1$ s. This is much shorter than the passage time of the fracture zone, $4\,\tau_A \approx 400$ s, and demonstrates that the internal

microphysics develops much more rapidly than the external conditions. This can mean, on the one hand, a great ability of the microprocesses to adjust to the changing internal parameters, but it also suggests that quantities that are not completely specified from the outside can be subject to severe changes. Among the latter we have to count, $j_{\parallel}$, n_F, T_F and the height extent Δh_F.

The dominant part of the energy converted in the fracture zone seems to appear as kinetic energy of the electron and ion beams, whereby the electrons carry most of the energy flux. Only a small fraction $(1 - \eta_b)$ is used up in the stochastic wave-particle interactions providing resistivity and maintaining a trapped particle population which guarantees charge neutrality in the presence of spatially varying positive and negative beam densities. The local dissipation rate is then:

$$\dot{u} = (1 - \eta_b)\eta^* j_{crit}^2 \quad . \tag{60}$$

With the above figures $\dot{u} \cong (1 - \eta_b)\ 10^2$ eV/(el). So, even if the parallel beams carry away more than 90% of the inflowing energy, we still expect heating rates of a few eV per particle and sec. The unperturbed temperature at 1 R_E altitude is of the order of 1 eV. It can be rapidly altered, if heat is not carried away by electron heat conduction. However, by the same process that reduces the electrical conductivity inside the fracture zone, also the thermal conductivity is dramatically reduced. The internally generated heat can escape only slowly by parallel heat conduction. This leads to pressure increase which drives the plasma out of the central fracture zone and causes *evacuation* in its interior and density enhancements at the upper and lower

borders. It is suggested that the density depletions observed above aurora [Benson and Calvert, 1979] result from this process.

We refrain from going into further details of these processes. Model calculations of the evacuation process have been performed and will be published. They show that within a few tens of seconds the density distribution over thousands of km can change by large factors. The drop in density can outweigh the rise of thermal velocity, so that j_{crit} is not increased by the heating and the current instability switched off. It is this chain of events which allows us to adopt the simple picture of an extended fracture zone inside which the current remains unstable for periods of several Alfvén travel times. But the unique values of n_F and c_{crit} appearing in the foregoing relations have no other meaning than to specify the initial current threshold when the fracture zone propagates into the unperturbed plasma. We then postulate that, whatever change of density, temperature, current density and height extent develops, the average j_{crit} through the fracture zone remains close to the initial value.

It may, however, well be that $j_{\parallel}$ becomes strongly structured. Splittings of auroral bands, exhibiting eastward and westward motions of the ray- or curl-structure which can be often seen in arcs observed in the magnetic zenith, may be the result of such current redistributions inside the fracture zone. The fast motions of rays and curls [Hallinan and Davis, 1970] by themselves are probably a result of a Kelvin-Helmholtz instability due to the strong shear flows on either side of the fracture zone (oppositely directed $E_{\perp}$, see Figures 1 and 2 in conjunction with the aforementioned density redistributions. The

detailed structure of so-called electrostatic shocks [Mozer et al., 1977] is by the same token affected by current redistributions.

Much work has to be done by theory and simulations, strongly guided by space observations, before all the complexities of the "fracture zone" are basically understood. Only when good models exist, can we attack the problem of Alfvén wave reflection quantitatively [Lysak, 1981; Lysak and Dum, 1983; Haerendel, 1983]. This explains the extremely simple approach to the problem of interaction between fracture zone and generator used in this paper and our reluctance to integrate the dynamic equation of the generator (Equation 37).

9. Summary

Auroral arcs appear to be the manifestation of a very common cosmic acceleration process [Haerendel, 1980, 1981, 1987, 1988]. It owes its existence to the release of strong magnetic shear stresses by violating, in thin sheets, the "frozen-in" condition of collisionless plasmas. Parallel voltages, on the one hand, decouple plasma at higher altitudes from the stellar surface (or atmosphere) and this way allow for a fast stress relief; on the other hand,they convert the released energy into parallel particle beams which quickly carry it out of the acceleration region. The parallel voltages are maintained by an effective resistivity created by instability of the field-aligned current. It turns out that knowledge of the magnitude of the resistivity is not needed for evaluation of the voltage. It is solely determined by the current threshold for instability, j_{crit}, the energy content per unit flux-tube and the propagation speed of the shear Alfvén waves which produce the stress release outside the acceleration region. The decisive quantity, the free magnetic energy per unit area stored in a magnetospheric-ionospheric current circuit, is defined by the integrated supercritical, field-aligned current density, i.e., j_{crit} and thickness, d. The thickness of auroral arcs is therefore energetically most significant. It reflects the strength of the generator or applied shear stresses, but not in a simple fashion. There is a matching problem related to differences in the bounce period of the oblique current sheets (Alfvén waves) and the acoustic eigenperiod of the generator. Non-perfect matching leads to multiple arc formation or brightness oscillations.

The whole energy release process, once initiated, can maintain itself by successive tapping of the energy reservoir, i.e., propagation of the acceleration

region into the current circuit, quite alike to the propagation of a fracture in a solid body. (In analogy with earthquakes, one could call the process also a "magnetic quake.") However, auroral arcs can also form under excessive energy pumping into the current circuit, so that it is forced to expand [Haerendel, 1987]. The propagation speed of an arc with respect to the plasma is given by the ratio of arc thickness and Alfvén travel time and is normally very slow. By contrast, very fast motions are set up in the stress release process above the fracture zone. They follow the direction of the shear stresses and are the reason for the great length of auroral arcs which typically exceeds their width by two orders of magnitude. They manifest themselves visibly in the fast motions of rayed structures [Hallinan and Davis, 1970]. The corresponding high transverse electric fields, which exist only at high altitudes, have been named "electrostatic" shocks by their discoverers [Mozer et al., 1977]. In the light of our interpretation they appear to be neither shocks, nor electrostatic, but nothing else than narrow (slightly) oblique current sheets which carry the message of a fracture in progress all along the involved flux-tubes, transform the magnetic energy into kinetic energy of the stress relief flow and feed the Poynting flux into the fracture zone. All of this has been cast into a set of simple physical relations, whose quantitative evaluation reproduces very realistic values for the observable quantities.

A completely different, but widely shared view of auroral acceleration is that it is essentially the mirror force acting on adiabatically moving hot electrons what sustains the field-aligned voltage in the presence of intense currents. We show that both processes can not only coexist and cooperate in producing the total voltage, the first one at heights of several 1000 km, the

second above about 2 R_E, but also that the small scales found in auroral arcs are quite compatible with the adiabatic current-voltage relation. This comes out of energy balance considerations and neglect of the weak coupling to the ionosphere. Most of the energy conversion, however, seems to occur in the fracture zone (higher resistance!), as well as most of the potential drop.

Kinetic corrections for describing the propagation of the crucial oblique current sheets do not appear to be necessary, except inside the generator and below the fracture zone. However, much work on the microprocesses evolving inside the fracture zone is necessary in order to understand the magnitude of the resistivity and many of the macroscopic consequences such as evacuation, current redistribution, heat flux and height extent of the parallel voltage. The evacuation is attributed, on the one hand, to anomalous heating, on the other hand, to a much reduced thermal conductivity which can lead to pressure build-up and plasma acceleration parallel to $\underline{B}$. The detailed exploration of all these micro- and macroscopic effects by experiment and theory continues to constitute one of the great challenges of space plasma physics.

ACKNOWLEDGEMENTS

This work was supported in part by the following grants: NASA NGL 16-001-043, NAGW-970, NSG-7632; and NSF ATM-8712236.

References

Antonova, Ye. Ye., and B. A. Tverskoy, Nature of the electron precipitation band of the "inverted V" type and of the Harang discontinuity in the evening sector of the auroral ionosphere, Geomagnetism and Aeronomy, 15, 85, 1975.

Armstrong, J. C., and A. J. Zmuda, Field-aligned current at 1100 km in the auroral region measured by satellite, J. Geophys. Res., 75, 7122, 1970.

Ashour-Abdalla, M., and C. F. Kennel, Nonconvective and convective electron cyclotron harmonic instabilities, J. Geophys. Res., 83, 1531, 1978.

Ashour-Abdalla, M., and R. M. Thorne, Toward a unified view of diffuse auroral precipitation, J. Geophys. Res., 83, 4755, 1978.

Benson, R. F., and W. Calvert, ISIS 1 observations at the source of auroral kilometric radiation, Geophys. Res. Lett., 6, 479, 1979.

Block, L. P., and C.-G. Fälthammar, Effects of field-aligned current on the structure of the ionosphere, J. Geophys. Res., 73, 4807, 1968.

Boström, R., H. Koskinen, and B. Holback, Low frequency waves and small-scale solitary structures observed by Viking, Proceedings 21st ESLAB Symposium, Bolkesjø, Norway, ESA SP-275, 185, 1987.

Carlqvist, P., and R. Boström, Space-charge regions above the aurora, J. Geophys. Res., 75, 7140, 1970.

Chiu, Y. T., A simple kinetic theory of auroral arc scales, J. Geophys. Res., 91, 204, 1986.

Chiu, Y. T., and J. M. Cornwall, Electrostatic model of a quiet auroral arc, J. Geophys. Res., 85, 543, 1980.

Cloutier, P. A., H. R. Anderson, P. J. Parks, R. R. Vondrak, R. J. Spiger, and B. R. Sandel, Detection of geomagnetically aligned currents associated with an auroral arc, J. Geophys. Res., 75, 2595, 1970.

Croley, D. R., Jr., P. F. Mizera, and J. F. Fennell, Signature of a parallel electric field in ion and electron distributions in velocity space, J. Geophys. Res., 83, 2701, 1978.

de la Beaujardiere, O., and R. Vondrak, Chatanika radar observations of the electrostatic potential distribution of an auroral arc, J. Geophys. Res., 87, 797, 1982.

Evans, D. S., Precipitating electron fluxes formed by a magnetic field-aligned potential difference, J. Geophys. Res., 79, 2853, 1974.

Evans, D. S., N. C. Maynard, J. Trøim, T. Jacobson, and A. Egeland, Auroral vector electric field and particle comparisons, 2. Electrodynamics of an arc, J. Geophys. Res., 82, 2235, 1977.

Fälthammar, C.-G., Generation mechanisms for magnetic field-aligned electric fields in the magnetosphere, J. Geomagnetism and Geoelectr., 30, 419, 1978.

Fennell, J. F., D. J. Gorney, and P. F. Mizera, Auroral particle distribution functions and their relationship to inverted Vs and auroral arcs, in Physics of Auroral Arc Formation, edited by S.-I. Akasofu and J. R. Kan, pp. 91-102, Geophysical Monograph 25, AGU, Washington D. C., 1981.

Frank, L A., and K. L. Ackerson, Observations of charged particle precipitation into the auroral zone, J. Geophys. Res., 76, 3612, 1971.

Fridman, M., and J. Lemaire, Relationship between auroral electron fluxes and field aligned electric potential difference, J. Geophys. Res., 85, 664, 1980.

Goertz, C. K., Kinetic Alfvén waves on auroral field lines, Planet. Space Sci., 32, 1387, 1984.

Goertz, C. K., and R. W. Boswell, Magnetosphere - ionosphere coupling, J. Geophys. Res., 84, 7239, 1979.

Gurnett, D. A., Electric field and plasma observations in the magnetosphere, in Critical Problems of Magnetospheric Physics, edited by E. R. Dyer, pp. 123-138, Nat. Academy of Sciences, Washington, D. C., 1972.

Haerendel, G., Auroral particle acceleration - an example of a universal plasma process, ESA Journal, 4, 197, 1980.

Haerendel, G., Magnetospheric processes possibly related to the origin of cosmic rays, in Origin of Cosmic Rays, edited by G. Setti, G. Spada, and A. W. Wolfendale, pp. 373-391, IAU Symposium No. 94, Reidel, Dordrecht, Holland, 1981.

Haerendel, G., An Alfvén wave model of auroral arcs, in High-Latitude Space Plasma Physics, edited by B. Hultqvist and T. Hagfors, pp. 515-535, Plenum, New York, 1983.

Haerendel, G., On the potential role of concentrated field-aligned currents in solar physics, Proc. 21st ESLAB Symposium, Bolkesjø, Norway, pp. 205-214, ESA SP-275, 1987.

Haerendel, G., Cosmic linear accelerators, submitted to Nature, 1988.

Hallinan, T. J., and T. N. Davis, Small-scale auroral arc distortions, Planet. Space Sci., 18, 1735, 1970.

Hasegawa, A., Particle acceleration by MHD surface wave and formation of aurora, J. Geophys. Res., 81, 5083, 1976.

Hudson, M. K., R. L. Lysak, and F. S. Mozer, Magnetic field-aligned potential drops due to electrostatic ion cyclotron turbulence, Geophys. Res. Lett., 5, 143, 1978.

Hudson, M. K., W. Lotko, I. Roth, and E. Witt, Solitary waves and double layers on auroral field lines, J. Geophys. Res., 88, 916, 1983.

Iijima, T., and T. A. Potemra, The amplitude of field-aligned currents at northern high latitudes observed by Triad, J. Geophys. Res., 81, 2165, 1976.

Kindel, J. M., and C. F. Kennel, Topside current instabilities, J. Geophys. Res., 76, 3055, 1971.

Knight, S., Parallel electric fields, Planet. Space Sci., 21, 741, 1973.

Lemaire, J., and M. Scherer, Ionosphere-plasma-sheet field-aligned currents and parallel electric fields, Planet. Space Sci., 22, 1485, 1974.

Lotko, W., Diffusive acceleration of auroral primaries, J. Geophys. Res., 91, 191, 1986.

Lyons, L. R., Generation of large-scale regions of auroral currents, electric potentials, and precipitation by the divergence of the convection electric field, J. Geophys. Res., 85, 17, 1980.

Lyons, L. R., Discrete aurora as the direct result of an inferred high-altitude generating potential distribution, J. Geophys. Res., 86, 1, 1981.

Lyons, L. R., D. S. Evans, and R. Lundin, An observed relation between magnetic field aligned electric fields and downward electron energy fluxes in the vicinity of auroral forms, J. Geophys. Res., 81, 457, 1979.

Lysak, R. L., Electron and ion acceleration by strong electrostatic turbulence, in Physics of Auroral Arc Formation, edited by S.-I. Akasofu and J. R. Kan, pp. 444-450, Geophysical Monograph 25, AGU, Washington D. C., 1981.

Lysak, R. L., and C. T. Dum, Dynamics of magnetospheric-ionospheric coupling including turbulent transport, J. Geophys. Res., 88, 365, 1983.

Mallinckrodt, A. J., and C. W. Carlson, Relations between transverse electric fields and field-aligned currents, J. Geophys. Res., 83, 1426, 1978.

Mozer, F. S., Anomalous resistivity and parallel electric fields, in Magnetospheric Particles and Fields, edited by B. M. McCormac, pp. 125-136, Reidel, Dordrecht-Holland, 1976.

Mozer, F. S., C. W. Carlson, M. K. Hudson, R. B. Torbert, B. Parady, J. Yatteau, and M. C. Kelley, Observations of paired electrostatic shocks in the polar magnetosphere, Phys. Rev. Lett., 38, 292, 1977.

Mozer, F. S., C. A. Cattell, M. K. Hudson, R. L. Lysak, M. Temerin, and R. B. Torbert, Satellite measurements and theories of low altitude auroral particle acceleration, Space Sci. Rev., 27, 155, 1980.

Papadopoulos, K., A review of anomalous resistivity for the ionosphere, Rev. Geophys. and Space Phys., 15, 113, 1977.

Parker, E. N., The dynamical properties of twisted ropes o f magnetic field and the vigor of new active regions on the sun, Ap. J., 191, 245, 1974.

Rowland, H. L.,P. J. Palmadesso, and K. Papadopoulos, One-dimensional direct current resistivity due to strong turbulence, Phys. Fluids, 24, 832, 1981.

Sagdeev, R. Z , and A. A. Galeev, Nonlinear Plasma Theory, Benjamin, N. Y., 1969.

Sato, T., A theory of quiet auroral arcs, J. Geophys. Res., 83, 1042, 1978.

Scholer, M., On the motion of artificial ion clouds in the magnetosphere, Planet. Space Sci., 18, 977, 1970.

Shelley, E. G., R. D. Sharp, and R. G. Johnson, Satellite observations of an ionospheric acceleration mechanism, Geophys. Res. Lett., 3, 654, 1976.

Swift, D. W., On the formation of auroral arcs and acceleration of auroral electrons, J. Geophys. Res., 80, 2096, 1975.

Swift, D. W., An equipotential model of auroral arcs, 2: numerical solutions, J. Geophys. Res., 81, 3935, 1976.

Swift, D. W., An equipotential model for auroral arcs: the theory of two-dimensional laminar electrostatic shocks, J. Geophys. Res., 84, 6427, 1979.

Temerin, M., K. Cerny, W. Lotko, and F. S. Mozer, Observations of double layers and solitary waves in the auroral plasma, Phys. Rev. Lett., 48, 1175, 1982.

Weimer, D. R., C. K. Goertz, D. A. Gurnett, N. C. Maynard, and J. L. Burch, Auroral zone electric fields from DE 1 and 2 at magnetic conjunctions, J. Geophys. Res., 90, 7479, 1985.

Whalen, B. A., and P. W. Daly, Do field-aligned auroral particle distributions imply acceleration by quasi-static parallel electric fields?, J. Geophys. Res., 84, 4175, 1979.

FIGURE CAPTIONS

Figure 1. A magnetospheric-ionospheric current circuit with generator near the equator and a magnetic fracture in progress at lower altitudes. The generator force, F_G, points out of the plane. Field-aligned currents, $j_\parallel$, sheared field component, $B_\perp$, unaffected convection speed, $v_\perp$, electric field, $E_\perp$, and are shown. The bell-shaped region of the enlarged fracture zone contains appreciable $E_\parallel \neq 0$. It propagates into the circuit and emits and reflects oblique current sheets traveling several times between fracture zone and generator and also, with much shorter period, between fracture zone and ionosphere (load region of the unperturbed current circuit). $E_\perp$ in the wave zone (inset) is typically one order of magnitude greater than the undisturbed field inside the circuit.

Figure 2. Fracture zone, attached oblique current sheets, ionosphere, generator and return (field-aligned) current shown in a simplified (homogeneous field) geometry. The divergences of generator current, J_G, and Pedersen current, J_p, correspond to sources and sinks of $j_\parallel$. Inside the (bell-shaped) fracture zone, $E_\parallel \neq 0$ and voltages of several kV exist over height ranges of several 1000 km. Electric equipotential lines are shown inside (horizontal) and adjacent to (vertical) this region. The slightly oblique (mostly field-aligned) currents above the fracture zone switch on and off strong

perpendicular electric fields, $\underline{E}_{\perp}$, which correspond to the stress relief motions, $v_{\perp}$, (out of plane). The fracture zone, whose width is of the order of 10 km, propagates into the current circuit (v_n) and is characterized by plasma evacuation in its interior and compression just on its outside.

Figure 3. Interface of the leading oblique current sheet with the generator. $\underline{E}_{\perp}$ and $\underline{v}_{\perp}$ grow as the sheet propagates with velocity, v_n, in x-direction.

Figure 4. Impact of magnetic stress relief on the generator plasma which gets accelerated (1-4), cools and is slowed down again (5-7) by the residual stresses. Eventually the motion is reversed (8). Kinks in the field-lines are points of intersection with the oblique current sheets of the previous figures. They propagate with Alfvén-speed, c_A.

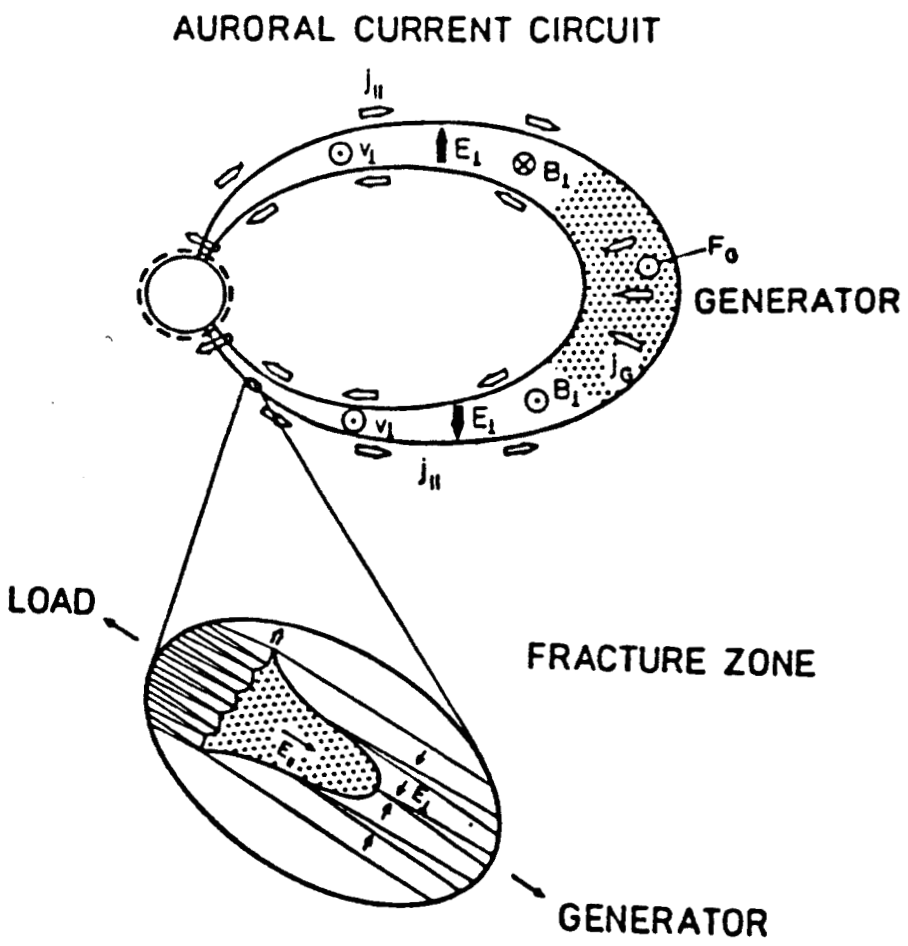
AURORAL CURRENT CIRCUIT
$j_{\parallel}$
$v_{\perp}$
$E_{\perp}$
$B_{\perp}$
F_0
GENERATOR
j_0
$B_{\perp}$
$v_{\perp}$
$E_{\perp}$
$j_{\parallel}$
LOAD
FRACTURE ZONE
$E_{\perp}$
$E_{\perp}$
GENERATOR

Figure 1

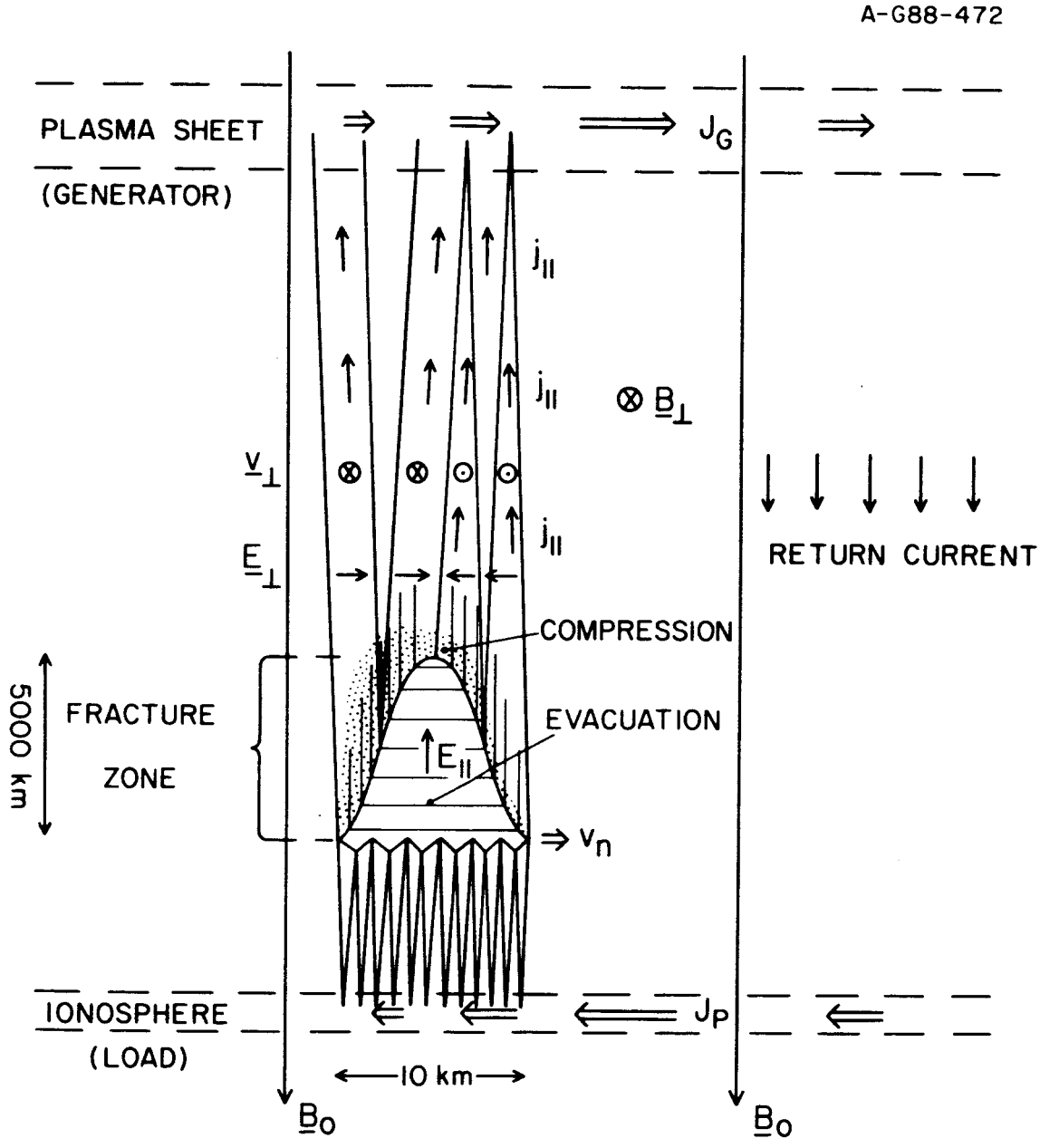
A-G88-472
PLASMA SHEET
(GENERATOR)
J_G
j_{II}
j_{II}
$\otimes \underline{B}_\perp$
$\underline{v}_\perp$
j_{II}
$\underline{E}_\perp$
RETURN CURRENT
COMPRESSION
5000 km
FRACTURE
ZONE
EVACUATION
E_{II}
$\Rightarrow v_n$
IONOSPHERE
(LOAD)
J_P
10 km
$\underline{B}_o$
$\underline{B}_o$

Figure 2

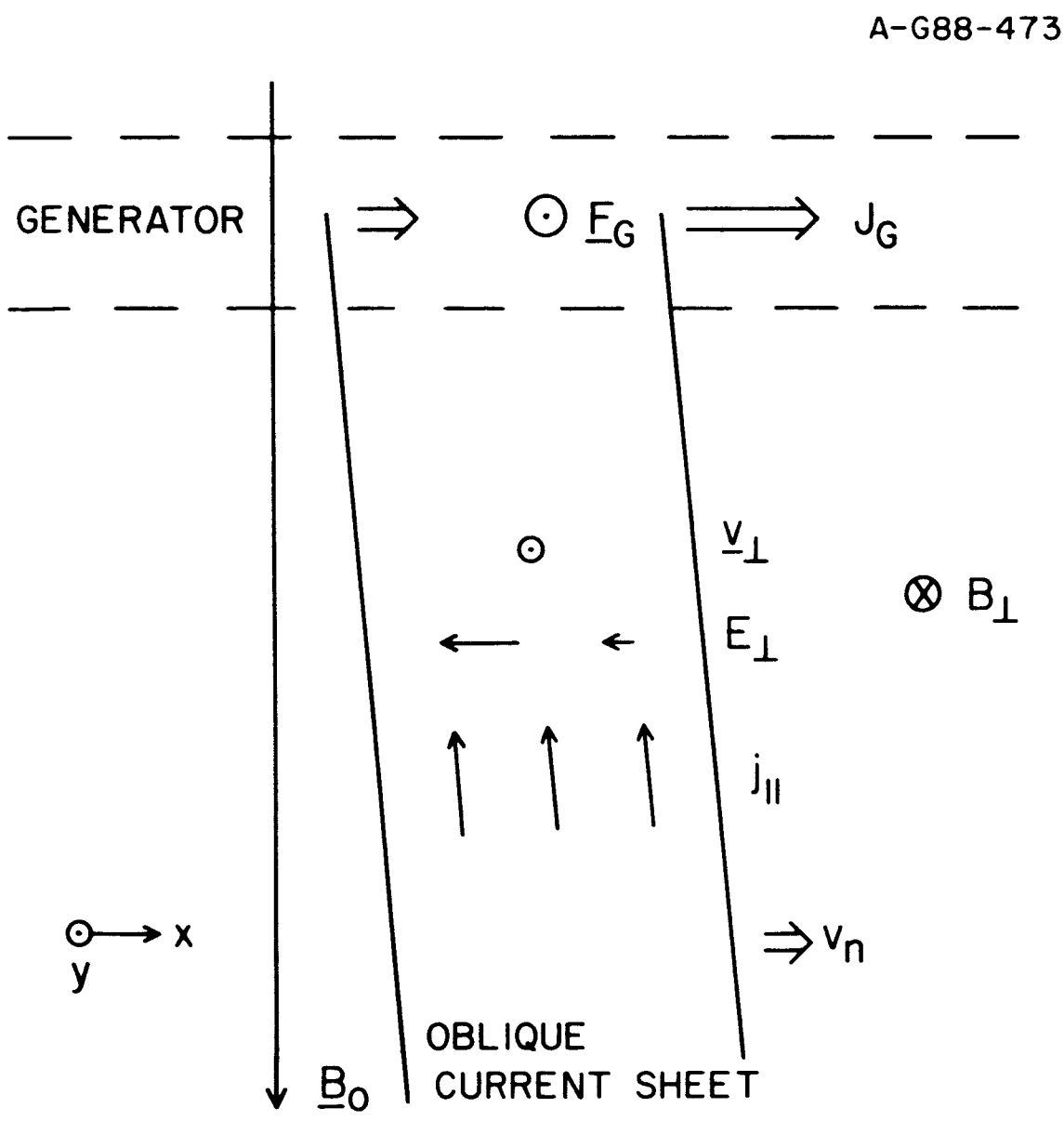
A-G88-473
GENERATOR
$\underline{F}_G$
J_G
$\underline{v}_\perp$
$B_\perp$
$E_\perp$
$j_\parallel$
x
y
v_n
OBLIQUE
CURRENT SHEET
$\underline{B}_0$

Figure 3

A-G88-471

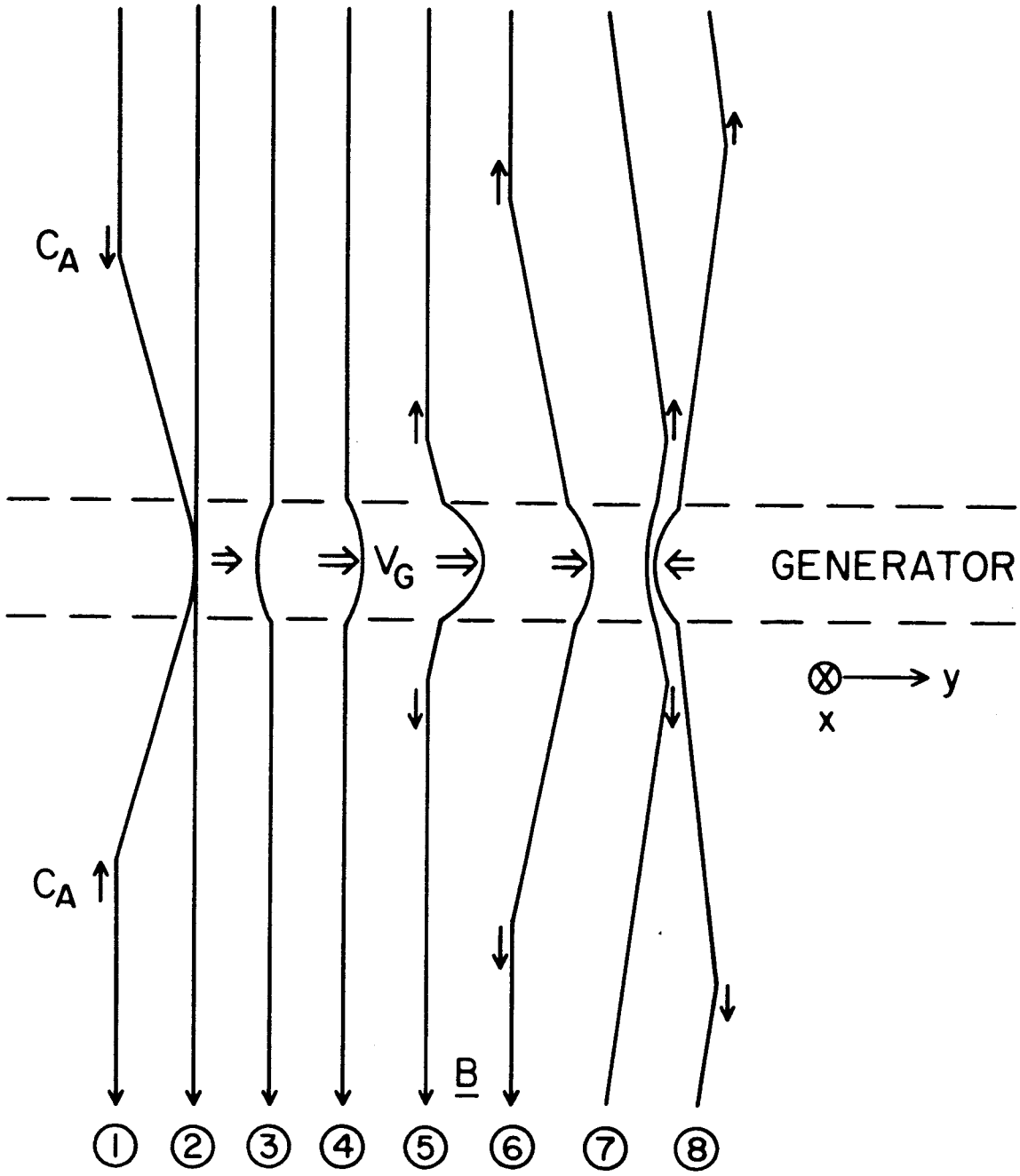

Figure 4